MARS BALLOON TRAJECTORY MODEL FOR MARS GEOSCIENCE AEROBOT DEVELOPMENT

Matthew Kuperus Heun
Jet Propulsion Laboratory
California Institute of Technology
Pasadena, California 91109

Henry M. Cathey, Jr.
Physical science Laboratory, New Mexico State University
NASA Wallops Flight Facility, Wallops Island, Virginia 23337

Robert Haberle
NASA Ames Research Center
Moffett Field, California 94035

Abstract

The Mars Geoscience Aerobot (MGA) is a proposed Mars aerobot (Aeronautical roBOT) mission featuring advanced capabilities for surface imaging and atmospheric science. The MGA consists of a superpressure balloon that is reflective on top and white on the bottom to avoid condensation of CO_2 frost during the night. The MGA also features a "smart" gondola with autonomous navigation capabilities.

Development of the Mars Balloon Trajectory Model (MBTM) has been an essential element of the planning and design of the MGA mission. This paper presents the balloon design and results from the MBTM, an integrated thermal, vertical, and trajectory model for balloon flight at Mars.

A promising design for the MGA involves a 27-m diameter, spherical, superpressure balloon, and a sophisticated science gondola weighing 15-30 kg. The balloon is designed to float more than 6.5 km above the planetary datum, and the MBTM shows that long-duration, 90-day missions are possible using advanced composite materials for the balloon envelope. Simulated trajectories show that several West-to-East transects are possible, covering hundreds of thousands of kilometers and more than 30 degrees latitude. Horizontal speeds range from a maximum of 80 m/s to a minimum of about 10 m/s with a nominal eastward velocity of nearly 40 m/s.

Introduction

Development of the Mars Geoscience Aerobot (MGA) mission has been catalyzed by science objectives that include surface geology and atmospheric measurements.

Of primary geologic interest is the nature and structure of water-lain deposits in the northern lowlands.[1] In terms of atmospheric science, measurements of temperature, pressure, winds, IR spectra of dust, and atmospheric constituents are planned. Global coverage is desired for comprehensive planetary characterization.

The MGA meets the above science objectives by providing an aerial vehicle from which atmospheric measurements can be made and detailed surface images can be obtained. The MGA carries a "smart" gondola with autonomous navigation capabilities that enable the acquisition of state-driven, sequenced, high-resolution images W on the ability to determine position, attitude, and velocity using celestial references, inertial sensors, and image data

Buoyancy for the MGA is provided by a superpressure balloon that is reflective on top and white on the bottom to avoid condensation of CO_2 frost during the night.

This paper provides the details of a model which predicts MGA trajectories, the MBTM. The predicted ground tracks are useful for evaluating the science potential from an aerobot flight. The Mars Balloon Trajectory Model (MBTM) was developed as part of a MGA feasibility study recently conducted by the Planetary Aerobot Program of the Jet Propulsion Laboratory in conjunction with NASA-Wallops Island, Lockheed-Martin Aerospace, CNES (France), and the space Dynamics Laboratory.

MGA Design

The design effort for the MGA balloon system was focused on (a) determining technical feasibility of an Aerobot/Balloon mission to Mars for the 2001 opportunity and (b) formulating a baseline mission concept. Many technical challenges were addressed to determine if a balloon system can be constructed that

will satisfy mission objectives. The balloon and system feasibility were baaed on a set of worst case conditions, from a balloon performance standpoint, that bound the engineering problem. Neck *et al.*[2] provide a general description of the entire system. The design approach for the balloon was similar to the efforts currently being employed for the development of a Long Duration Balloon Vehicle by NASA's Balloon Programs Branch.

Design Considerations

There are several considerations that influenced the MGA design in general and the balloon envelope in particular. The primary considerations for the balloon design are the type of balloon to be flown, the thermal/radiative environment, the envelope materials, the balloon sire, the storage options, the deployment mechanism, the inflation technique, the super pressure flight environment and mass and volume constraints. The balloon deployment/inflation strategy, envelope reefing, aerodynamic stability, deceleration sequence, tank location and inflation direction all contribute to the resulting design. The details of the dependencies and interdependencies of the system design are detailed in a paper Smith *et al.*[3]

The two primary considerations that dictate a majority of the design requirements are the balloon material design and the thermal environment to which the balloon is exposed An existing "off-the-shelf' balloon material which will meet at] system requirements does not exist. A key factor was the strength to weight ratio of the balloon material. The material design considerations for the development of this new balloon material included strength, creep, areal density, fracture toughness, static charging, low temperature behavior, permeability, pinholing, seaming, fabrication folding, radiative optical properties, exposure degradation, and sterilization.

Both cylindrical and spherical balloons were reviewed for the system mass and required material strength versus float altitude, and a spherical superpressure balloon made of a composite material was selected as the design which best meets the mission requirements. The mission requirements dictated a high strength, low mass, and gas impermeable structure. The composite was designed with four different materials: scrim, Mylar, polyethylene, and adhesive. The Kevlar scrim provides strength with very light weight, the Mylar provides substrate stiffness and a gas barrier, the polyethylene provides pinholing resistance, fracture toughness, and a second layer of gas barrier, and the adhesive bonds and adds additional pinholing resistance. The film strength requirement evolves from day/night pressure variations which are a function of thermal loading. Figure 1 presents the thermal environment exposure. The final design specifications of the MGA balloon that demonstrate technical feasibility are as follows:

Spherical Superpressure Balloon
Volume = 10,500 m^3
Diameter = 27.17 m
Balloon mass = 55 kg
Gas Mass = 12 kg
Payload = 15-30 kg
Float altitude = 6.5-12 km
Daytime ΔP = 240 Pa
Nighttime ΔP = 20 Pa

Solid Carbon Dioxide Deposition

Review of the worst-case environmental conditions showed the possibility that solid Carbon Dioxide may deposit on the balloon at night in a Martian atmosphere. Condensation is detrimental to the balloon performance because it adds mass to the system and degrades the optical-radiative properties of the balloon envelope. Both conditions significantly reduce the flight duration. The overall energy balance and coupling to its environment determines the object's steady state temperature and the potential for condensation. The thermal loads are from direct sunlight, reflected sunlight (off of the planet), and scattered sunlight due to particulate matter in the atmosphere. The heat rejection (or absorption) is via radiation to either the atmosphere above the balloon (canopy) or to/from the atmosphere below the balloon (floor). The Mars environmental models provide characteristics for these radiation sources.

The balloon nighttime temperature relation can be written in a form that uses canopy and floor temperatures, the effective upper sky and lower atmosphere radiative temperatures, respectively. The floor and canopy temperatures are derived from the nighttime IR fluxes given by the Mars atmospheric models by the following:

$$T_{floor} = \left(\frac{q''_{IR,diffuse,upward}}{\sigma} \right)^{0.25}, \qquad (1)$$

and

$$T_{canopy} = \left(\frac{q''_{IR,diffuse,downward}}{\sigma} \right)^{0.25}. \qquad (2)$$

Neglecting convection (a good assumption due to Mars' thin atmosphere) and assuming steady state, the nighttime balloon skin temperature is a function of the environmental conditions and the ratio of emissivities on the top and bottom of the balloon.

$$T_{film} = \left(\frac{T_{floor}^4 + \frac{\varepsilon_{top}}{\varepsilon_{bot}} T_{canopy}^4}{1 + \frac{\varepsilon_{top}}{\varepsilon_{bot}}} \right)^{0.25} \quad (3)$$

The nighttime balloon temperature will reach a steady state-temperature at a point between the floor and canopy temperatures. If a balloon were to have surface properties that are consistent *over the* entire surface ($\varepsilon_{top} = \varepsilon_{bot}$), then Equation 3 becomes simply

$$T_{film} = \left(\frac{T_{floor}^4 + T_{canopy}^4}{2} \right)^{0.25} , \quad (4)$$

and the steady-state film temperature is independent of the emissivity of the film. For a balloon with different emissivities on the top and the bottom of the balloon, the nighttime steady state film temperature can be raised or lowered by adjusting the emissivity ratio,

Gaseous Carbon Dioxide will condense (sublimate) to a solid on the balloon if the temperature of the balloon falls below the local saturation temperature for CO_2 ($T_{film} < T_{sat}$). The state of the CO_2 is a function of the ambient pressure as given by the saturation pressure-temperature phase relationship. Figure 2 shows the relationship between the saturation curve and the balloon temperatures.'

The nighttime steady state flight temperature is close to the solid/vapor line. To move away from this line and to provide margin, the balloon's temperature must be increased, or the saturation temperature must be decreased. The nighttime balloon temperature can be increased by adjusting the emissivity ratio as discussed above. The saturation temperature can be decreased by reducing the ambient pressure by moving to a higher float altitude. In Figure 3 the CO_2 condensation temperature is plotted as a function of altitude for the BLM environment. Notably, there is little effect of altitude on the saturation temperature. Thus, simply flying the balloon higher will not significantly reduce the temperature margin above the sublimation point. Furthermore, an altitude change does not provide significant change in the nighttime steady state balloon temperature.

The radiation coupling can be changed by either increasing radiation coupling of the balloon to the warmer source (the planet's surface) or by decreasing radiation coupling of the balloon to the colder source (the sky). For the Mars balloon, it is desired to make the balloon temperature closer to the floor temperature. The recommended method of increasing the balloon temperature is to have different emissivities for the top and bottom of the balloon. The desired thermal optical properties for the Mars balloon are to have a low a and low ε for the top surface and a low a and high ε for the bottom surface.

The balloon would keep most of the heat given off by the planet with minimal radiation back into space. Two different configurations that satisfy these requirements have been identified. The first is a balloon which is white on the bottom and metalized on the top. The second is a balloon which is "semi-transparent" on the bottom and metalized on the top. The "semi-transparent" material is could be the proposed laminated film with no other surface treatments. The emissivity ratios are shown in the figures

Figure 4 shows the balloon equilibrium temperature in addition to the floor and Carbon Dioxide saturation temperatures. One line shows a balloon with a white surface top and bottom. It is seen that such a balloon is perilously close to the CO_2 solid/vapor transition temperature. Another curve shows a balloon with a white surface on the bottom and an aluminized top (aluminum side out). A considerable temperature margin is gained over the CO_2 condensation line with such a balloon configuration. Finally, an aluminized top (aluminum side out) and clear bottom (Mylar/PE/Kevlar scrim) balloon is shown.

It has been shown that deposition of solid Carbon Dioxide on the balloon at nighttime is a potential problem, but it can be effectively mitigated The nighttime float condition is marginally near the vapor state side of the solid/vapor line. This implies that all of the Carbon Dioxide will remain in the gaseous state. It is anticipated that there will be no condensation of the Carbon Dioxide on the balloon at the stated float conditions. The emissivity of the top and bottom of the balloon can be changed to provide an increased margin over the estimated float temperature

Mars General Circulation Model (GCM)

The Mars General Circulation Model (Mars GCM) grew from an Earth weather model in the late 1960s. It simulates the dynamics of the Martian atmosphere on a global scale, much like weather models for the Earth. Atmospheric parameters available from the GCM include winds, solar radiation (direct, upward diffuse, and downward diffuse), infrared radiation (upward and downward), temperature, pressure, and topography. Initially, the Mars GCM modeled only two vertical layers in the atmosphere. As the cost of computational power decreased, improved vertical and horizontal resolution was added to the GCM. Topographic effects have been included. The Mars GCM now models the effect of dust on radiation dust-wind interactions, and the seasonal sublimation patterns of the polar ice caps.[5]

The Mars GCM requires several inputs including (a) the initial solar longitude L_s, (b) the total mass of the atmosphere, (c) the total atmospheric dust load, (d) the distribution of surface thermal inertia, (e) the distribution of planetary albedo, and (f) the assumed ratio of the atmospheric optical depth in the IR wavelengths to the atmospheric optical depth in the solar wavelengths, τ_{IR}/τ_{sol}. Viking data guided the selection of inputs for the GCM runs employed in the MGA simulations shown herein. For example, the total mass of the atmosphere was selected such that the predicted seasonal surface pressure variations match the Viking measurements.[6]

GCM Output

The GCM output used for predicting MGA trajectories is arranged in a planetary grid upon which atmospheric parameters are reported. The following parameters are given at each gridpoint:

- atmospheric temperature, T_{atm},
- surface pressure, P_{surf},
- the solar zenith angle, ζ,
- direct solar flux, q''_{sol},
- downward diffuse solar flux, $q''_{sol,diffuse,downward}$,
- upward diffuse solar flux, $q''_{sol,diffuse,upward}$,
- downward IR flux, $q''_{IR,diffuse,downward}$,
- upward IR flux, $q''_{IR,diffuse,upward}$,
- the east-west wind component u_{wind}, and
- the north-south wind component v_{wind}.

The pressure at any attitude z can be calculated by

$$P(z) = P_{surf}\, e^{-(z-z_{surf})/H} \tag{5}$$

where H is the atmospheric scale height, taken to be 11.18 km, and z_{surf} is the surface altitude.

The GCM spatial grid contains 7 vertical divisions (up to about 10 km above the planet's surface), 40 longitude divisions, and 25 latitude divisions. The parameter grid is updated sixteen times per Martian day.

MGA Balloon Model

Flight trajectory prediction is an integral part of MGA mission development, because the expected flight profiles (a) determine which parts of Mars can be reasonably explored by balloon, (b) drive the balloon design, and (c) are useful for science sequencing and navigational crosschecks once in flight.

The model for MGA motion is a set of ordinary differential equations (ODES) that describe the time-evolving behavior of the balloon System."* The GCM provides the environmental input parameters for the MGA model.

Equations of motion

Four ODES describe the horizontal and vertical motion of the balloon.

Horizontal motion

The balloon is assumed to have zero horizontal acceleration, and it flies with the winds. Accounting for the curvature of the planet, the change of longitude (in degrees) with time is given by

$$\frac{d(lon)}{dt} = \frac{180}{\pi(R_M + z)\cos(lat)}\, u_{wind} \tag{6}$$

The change in latitude with time is given by

$$\frac{d(lat)}{dt} = \frac{180}{\pi(R_M + z)}\, v_{wind} \tag{7}$$

Both u_{wind} and v_{wind} are provided by the GCM for a given time and balloon location. R_M is the mean radius of Mars, taken to be 3393.5 km.

Vertical motion

The change in vertical position z with time is

$$\frac{dz}{dt} = w, \tag{8}$$

and the change in vertical velocity w with time is given by

$$\frac{dw}{dt} = a_z. \tag{9}$$

The balloon vertical acceleration a_z is found by summing the forces on the system,

$$(m_{act} + m_{virt})a_z = F_{grav} + F_{buoy} + F_{drag}. \tag{10}$$

where

$$m_{act} = m_{hdw} + m_{gas}, \tag{11}$$

$$m_{virt} = C_{vm}\rho_{atm} V g_M, \tag{12}$$

and

$$m_{hdw} = m_{film} + m_{gond} + m_{misc}. \tag{13}$$

The miscellaneous mass m_{misc} includes tethers, load tapes, fill plugs, and other items. The forces are given by

$$F_{grav} = m_{act} g_M, \tag{14}$$

$$F_{buoy} = \rho_{atm} V g_M, \tag{15}$$

and

$$F_{drag} = C_D A_x \frac{1}{2}\rho_{atm}(-w)|w|. \tag{16}$$

Following custom,[8] the coefficient of virtual mass C_{vm} is taken to be 0.5. The drag coefficient CD is 0.8, and the balloon dimensional parameters are given by

$$AX = \frac{\pi}{4}D^2, \tag{17}$$

$$V = \frac{\pi}{6}D^3, \tag{18}$$

and

$$S = \pi D^2. \quad (19)$$

The acceleration due to gravity at Mars g_M is 0.38 that of earth or 3.73 m/s^2.

Thermodynamic equations

Three ODES describe the thermodynamic evolution of the balloon. The lifting gas and film are each modeled as a single node. First, the mass balance for the lifting gas is given by the leak rate/ which is, in general, a function of time, superpressure level, balloon skin temperature, and other factors.

$$\frac{d(m_{gas})}{dt} = -\ell \quad (20)$$

Accounting for gas leakage, the energy balance on the balloon gas is given by

$$\frac{d(mC_vT)_{gas}}{dt} = -q_{conv,is} - C_{p,gas}T_{gas}. \quad (21)$$

Because the MGA has a constant-volume superpressure balloon, there is no volume change term in Equation 21. The energy balance for the balloon film is given by the following equation.

$$\frac{d(mCT)_{film}}{dt} = q_{conv,os} + q_{conv,is} + q_{solar,direct,top} + q_{solar,direct,bot} + q_{solar,diffuse,top} + q_{solar,diffuse,bot} + q_{IR,top} + q_{IR,bot} \quad (22)$$

The gas properties $C_{p,gas}$ and $C_{v,gas}$ are, in general, a function of the gas state.

Heat transfer

The various heat transfer terms in Equations 21 and 22 are given below.

$$q_{conv,os} = h_{os}S(T_{atm} - T_{film}) \quad (23)$$

$$q_{conv,is} = h_{is}S(T_{gas} - T_{film}) \quad (24)$$

$$q_{solar,direct,top} = \alpha_{top}A_{x,top}q''_{sol} \quad (25)$$

$$q_{solar,direct,bot} = \alpha_{bot}A_{x,bot}q''_{sol} \quad (26)$$

$$q_{solar,diffuse,top} = \alpha_{top}\frac{S}{2}q''_{sol,diffuse,downward} \quad (27)$$

$$q_{solar,diffuse,bot} = \alpha_{bot}\frac{S}{2}q''_{sol,diffuse,upward} \quad (28)$$

$$q_{IR,bot} = \varepsilon_{bot}\sigma\frac{S}{2}\left(T^4_{canopy} - T^4_{film}\right) \quad (29)$$

$$q_{IR,bot} = \varepsilon_{bot}\sigma\frac{S}{2}\left(T^4_{floor} - T^4_{film}\right) \quad (30)$$

The cross-section area of the top and bottom surfaces are a function of the zenith angle of the sun ζ.

$$A_{x,top} = \frac{\pi}{8}D^2(1 + \cos(\zeta)) \quad (31)$$

$$A_{x,bot} = \frac{\pi}{8}D^2(1 - \cos(\zeta)) \quad (32)$$

The canopy temperature, the floor temperature, the direct solar flux, the diffuse solar flux, and the solar zenith angle are given by the GCM as a function of time and position. The solar absorptivities and IR emissivities of the top and bottom portions of the balloon skin area function of the balloon coating.

Finally, the convective heat transfer coefficients h_{os} and h. are given by standard Nusselt number correlations for spherical surfaces. The Nusselt numbers are a function of the relative vertical velocity of the balloon and the properties of the atmospheric gas and internal gas.

Solving the system of equations

The system described by Equations 1 through 32 represents a well-posed set of seven ordinary differential equations. Given initial conditions on all the variables of interest (lon, lat, z, w, m_{gas}, T_{gas}, and T_{film}), one can find the time-evolving behavior of the balloon and present the position, velocity, and thermodynamic state of the system as a function of time.

Standard numerical integration routines can be used to solve the system of equations. There are no special considerations for the numerical integration step size because the system is relatively well-behaved and evolves slowly with time.

Sample MGA trajectories

Simulation assumptions and initial conditions

The MGA trajectories presented herein use atmospheric data provided by the Mars GCM. As stated above, the inputs to the GCM were selected such that the GCM predictions match data gathered by the Viking landers.

The initial conditions for the MGA trajectory presented herein are:

$$L_s = 220°, \quad (33)$$

$$\text{Longitude} = 110° \text{ W}, \quad (34)$$

$$\text{Latitude} = 55° \text{ N}, \quad (35)$$

$$z = 3000 \text{ m}, \quad (36)$$

$$w = 0 \text{ m/s}, \quad (37)$$

$$T_{film} = T_{atm}, \quad (38)$$

$$T_{gas} = T_{atm}, \quad (39)$$

and

$$m_{gas} = 12 \text{ kg}. \quad (40)$$

The Mars GCM run that was used for the trajectory predictions begins at $L_s = 220°$ and has $\tau_{IR} = \tau_{sol}$.

Surface coverage

Figures 5 and 6 show two projections of the ground track of the MGA. The ground track is

determined by the winds at float altitude. There are two regimes of aerobot flight shown in this simulation. During the first part of the flight, the aerobot is in the northern hemisphere, and the dominant winds drive the MGA eastward. The aerobot provides several circumnavigating transects of the planet. Note, however, that a small southward wind component exists, and the aerobot is driven slowly southward as it encircles the planet. Each circumnavigation takes about 5 days at 30° latitude.

A flight regime transition occurs as the aerobot approaches equator. The southward component of the wind becomes stronger, and the aerobot reaches the southern hemisphere. As the MGA approaches the equator, surface elevations become dangerously high, and it is necessary to jettison some ballast. After 15 kg of ballast is released, the aerobot flies safely across the equator into its second flight regime.

During the last 40 days of the flight, the balloon experiences *very* quiescent winds. The surface velocity decreases, but excellent imaging and science opportunities are available for the area beneath the aerobot. Finally, northward winds drive the MGA toward the equator again where it impacts some mountains, 92 days after deployment.

Figure 7 shows the ground track velocity (the apparent velocity of the MGA as it traverses the surface) for this particular flight, The ground track velocity is as high as 80 m/s early in the flight when the aerobot is circling the planet. Later in the flight when quiescent winds are experienced, the velocity drops to less than 10 rids.

Seasonal variations in the wind patterns can alter the ground track significantly. Several simulations performed for a Mars Aerial Platform (MAP) proposal show similar west-to-east paths.[9]

Vertical Profile

Because the MGA is a superpressure balloon, its vertical trajectory is determined by variations in the atmospheric density profile. In the absence of gas leaks, a superpressure balloon's system mass and volume (and therefore overall density) remain constant during a flight, The balloon always seeks its constant density altitude in the atmosphere. Thus, variations in the atmospheric pressure and temperature profile affect the balloon's vertical position.

There are both seasonal and diurnal time scales to atmospheric pressure variation, On a seasonal time scale, the atmospheric pressure profile is influenced by Mars' orbital eccentricity. During the southern hemisphere summer ($270° \leq L_s < 3600$), Mars is closer to the sun than during the northern hemisphere summer ($90° \leq L_s < 1800$). The higher solar heat flux associated with the shorter Sun-Mars range during southern hemisphere summer results in additional sublimation of the southern polar ice cap and more gas in the atmosphere. Thus, the planetary-wide surface pressure is higher during southern summer than northern summer.

Higher atmospheric pressure leads to higher float altitudes, all other factors being equal. The result can be up to 2 km of seasonal float altitude variation for a given aerobot system design due to seasonal atmospheric pressure variations alone.

On diurnal time scales, Mars' pressure profile varies only slightly, less than 10??o per day. The diurnal pressure variations are the result of the passage of weather systems.

In contrast to atmospheric pressure variations, Mars' atmospheric temperature exhibit significant seasonal *and* diurnal variation. Typically, atmospheric temperature changes have the biggest impact on balloon vertical position.

On the seasonal time scale, higher temperatures and lower atmospheric density exist during summer than during winter. Thus, summer float altitudes will be lower than winter float altitudes in the absence of other effects.

On diurnal time scales, the atmospheric temperature varies less than 10 K at reasonable float altitudes. During the day, the balloon will sink slightly as the atmosphere becomes less dense with increasing temperature. At night, balloon float altitudes are higher as due to atmospheric cooling and increased density.

Figure 8 shows the vertical profile for this flight, The diurnal variation of float altitude is noticeable. Night altitudes are somewhat higher than day altitudes as discussed above. Note also that the ballast drop produces an initial altitude increase to get over some mountains. Soon after the ballast drop, however the altitude decreases as the aerobot encounters the warmer conditions near the equator. Seasonal (and therefore hemispherical) weather variations are shown to play an important role in the vertical flight profile of the aerobot

Ideally, the aerobot should fly near the Martian surface to obtain high-resolution images. Clearly, the wide variation of Martian topography provides a severe challenge for aerobot designers and scientists Ballast options can provide a long-lasting robust system with the capability of crossing the high equatorial mountains at Mars.

Figures 5–8 show that the aerobot provides rich potential for high-resolution planet-wide surface imaging science. Global wind patterns and seasonal weather patterns supply ample planetary coverage for a lighter-than-air aerobot.

Conclusion

The above results show that a Mars aerobot mission is feasible and provides significant opportunity for planetary science. An aerobot can be designed for worst-case atmospheric conditions, and CO_2 frost accumulation can be mitigated. Numerous planet-encircling transects are possible over a 90-day flight.

High levels of uncertainty exist for the Mars atmosphere and topography. The uncertainty in the Martian atmosphere leads to difficulties in balloon design. A balloon designed for worst-case conditions (in terms of atmospheric temperature and pressure) will fly unsuitably high when placed in an atmosphere with nominal pressure and temperature characteristics. For example, a balloon designed for the lowest expected surface pressure may fly 1-2 km higher at off-design conditions (e g. another time of year with nominal conditions). Longduration aerobot flights provide a technical challenge that may be solved by carrying extra ballast which would be useful in a favorable atmosphere. If the aerobot encounters a nominal or unfavorable atmosphere, ballast could be dropped as described in the example mission presented above.

Acknowledgments

The work described in this paper was carried out by the Jet Propulsion Laboratory, California Institute of Technology, and by the Physical Science Laboratory, New Mexico State University, under contracts with the National Aeronautics and Space Administration.

References

1. Tanaka, K.L. *et* al. "Development of a Geoscience-Based Mission Strategy for an Aerobot Traverse of the Martian Northern Plains", International Conference on Mobile Planetary Robots & Rover Roundup, Santa Monica, California, 1997.

2. Nock, K.T. *et al. "Overview* of a Mars 2001 Aerobot/Balloon System". 12* AIAA Lighter-Than-Air Technology Conference, San Francisco, California, 3-5 June 1997.

3. Smith, 1.S. et al. "The Mars 2001 Balloon Design". 12* AIAA Lighter-Than-Air Technology Conference, San Francisco, California, 3-5 June 1997.

4. Dushman & Lafferty. *Scientific Foundations of Vacuum Technique.* p. *727,* J. Wiley and Sons, 1966.

5. Pollack, J.B. *et* al. "Simulations of the General Circulation of the Martian Atmosphere—1. Polar Processes". *Journal of Geophysical Research,* Vol. *95,* No. *B2,* pp. *1447-1473, 1990.*

6. Schaeffer, J. Personal communication, March *1996.*

7. L.A. Carlson & W.J. Horn. '*New Thermal and Trajectory Model for High-Altitude Balloons". *Journal of Aircraft,* Vol. *20, No. 6,* pp. 500-507, 1983.

8. Wu, J.J. & J.A. Jones. "Performance Model for Reversible Fluid Balloons", 11th AIAA Lighter-Than-Air Technology Conference, Clearwater Florida, 16-18 May 1995.

9. Greeley, *R. et al. Mars Aerial Platform (MAP).* Proposal submitted to NASA's Discovery Program 1994.

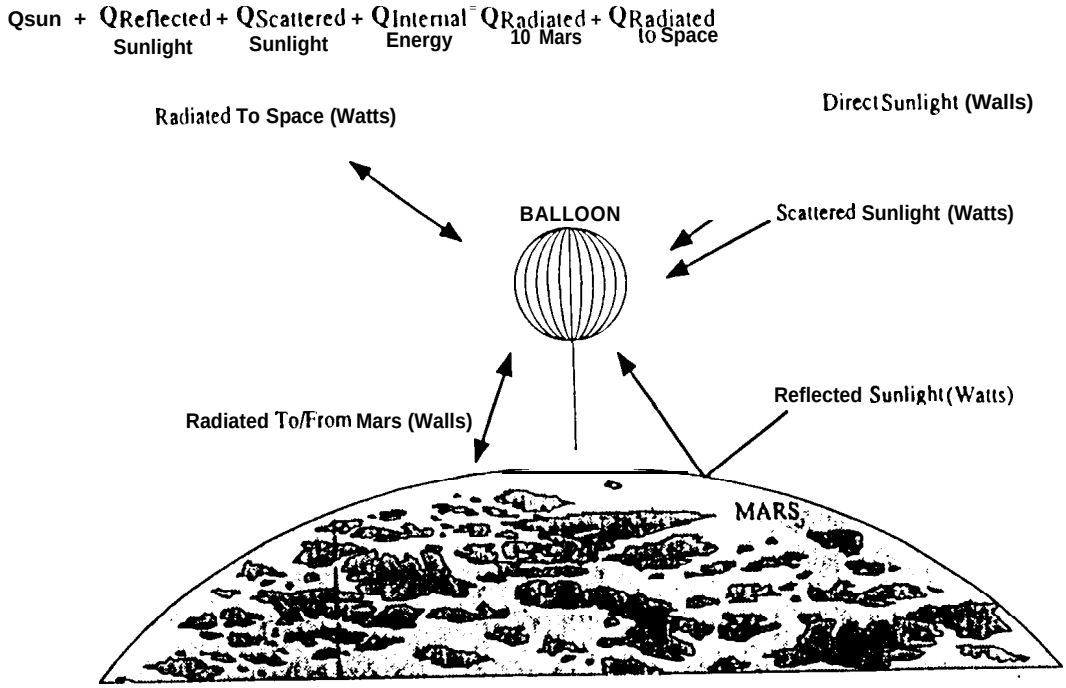

Figure 1. Balloon environment.

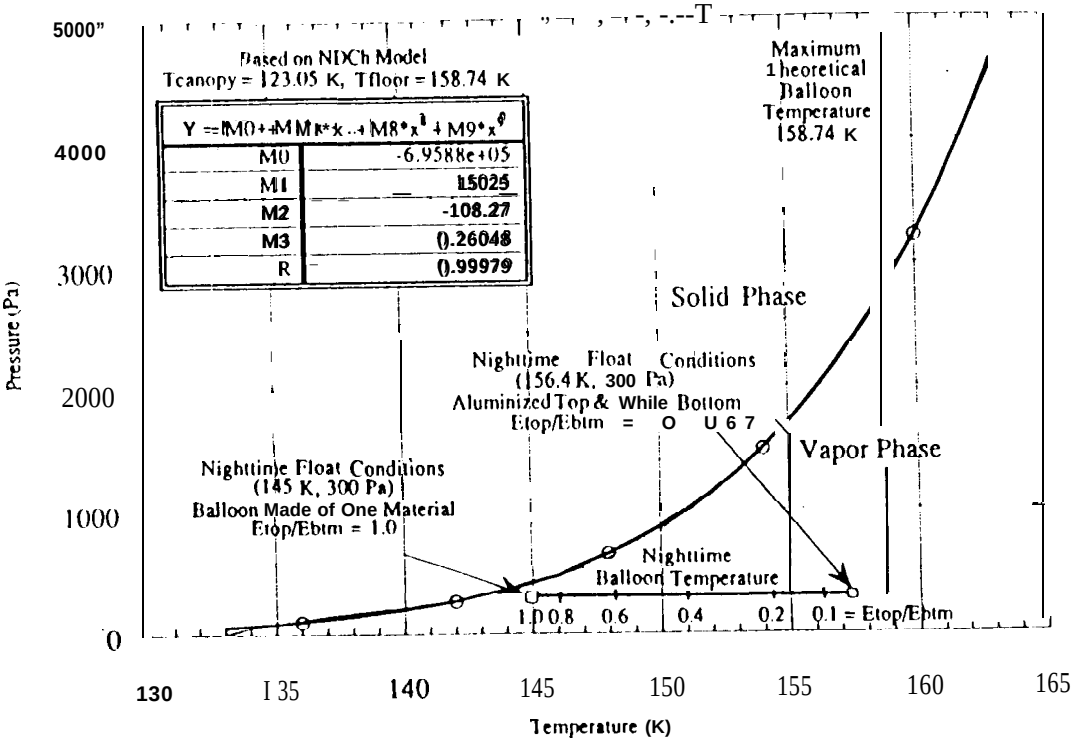

Figure 2. CO_2 saturation.

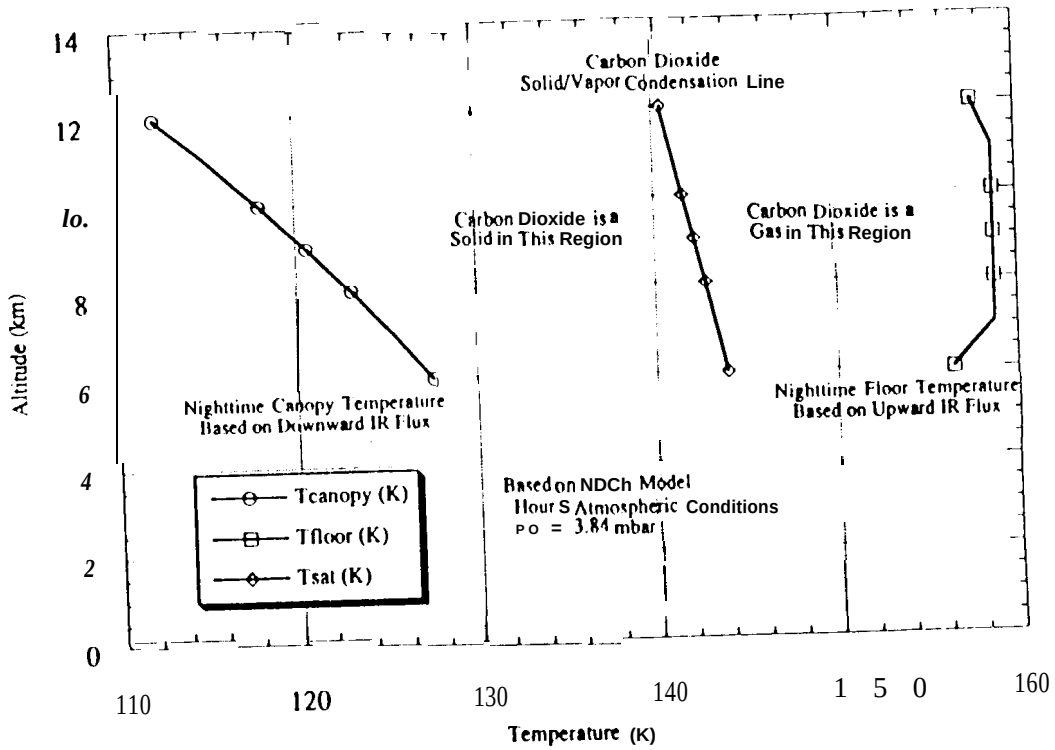

Figure 3. $C0_2$ saturation vs. altitude.

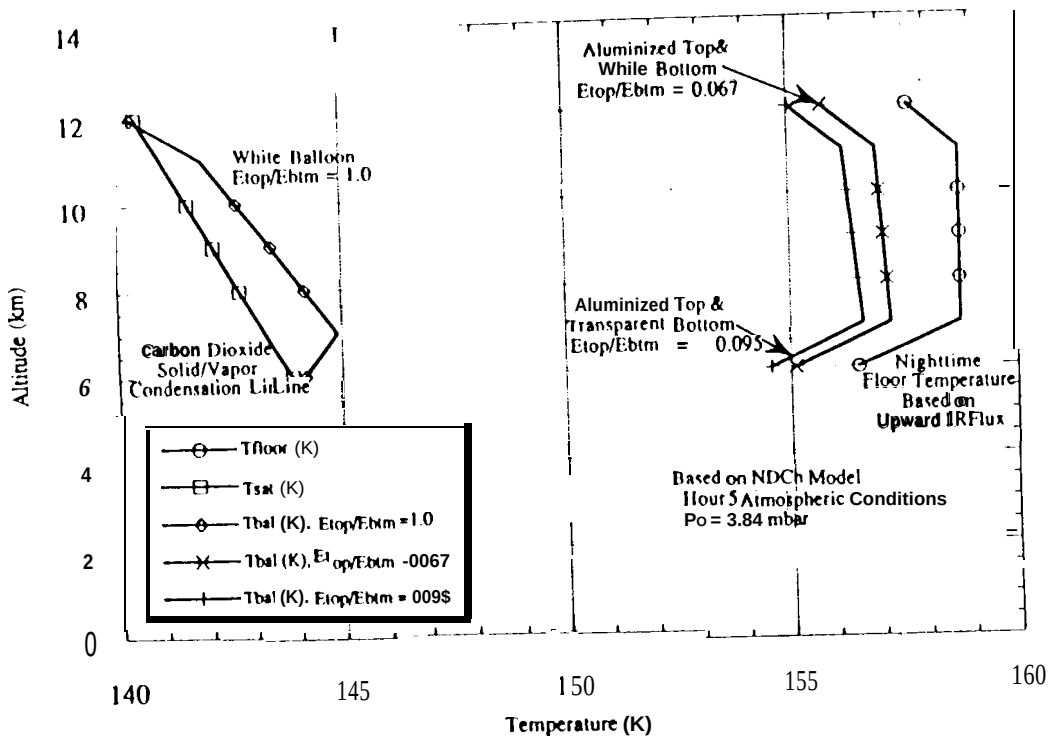

Figure *4.* Balloon and saturation temperatures.

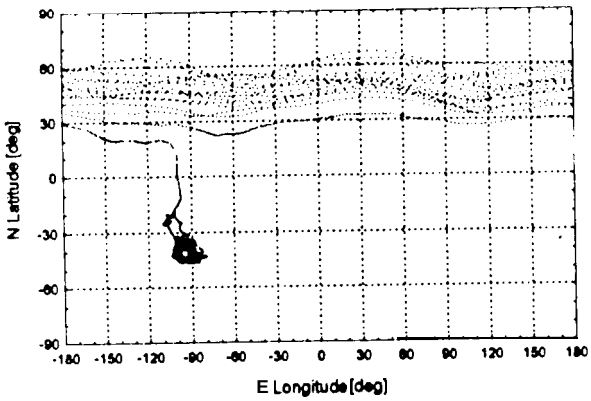

Figure 5. Aerobot ground track

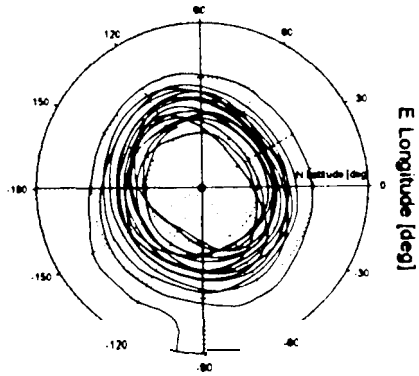

Figure 6. Aerobot ground track (polar projection).

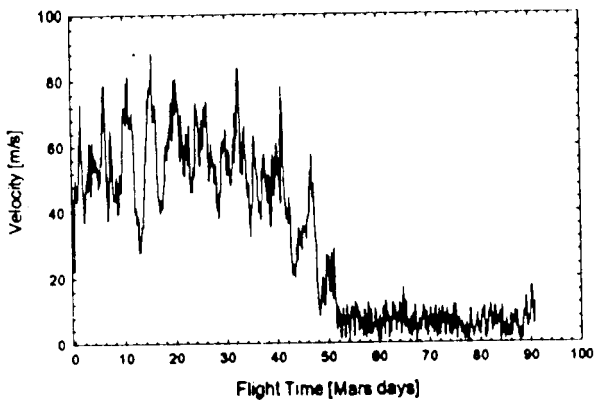

Figure 7. Aerobot velocity.

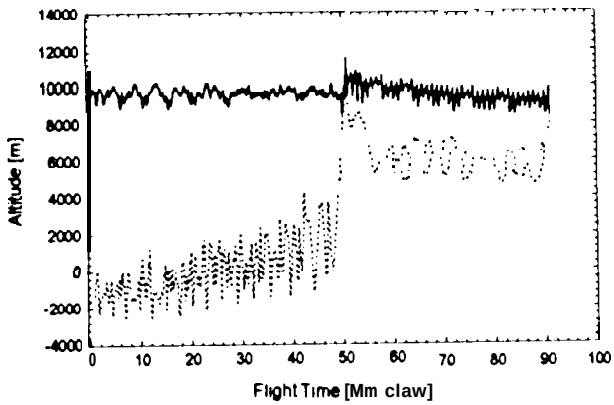

Figure 8. Vertical profile.